

Combined hardening and softening constitutive model of plasticity: precursor to shear slip line failure

A. Ibrahimbegovic, D. Brancherie

88

Abstract In this work, we present a finite element model capable of describing both the plastic deformation which accumulates during the hardening phase as the precursor to failure and the failure process leading to softening phenomena induced by shear slip lines. This is achieved by activating subsequently hardening and softening mechanisms with the localization condition which separates them. The chosen model problem of von Mises plasticity is addressed in detail, along with particular combination of mixed and enhanced finite element approximations which are selected to control the locking phenomena and guarantee mesh-invariant computation of plastic dissipation. Several numerical simulations are presented in order to illustrate the ability of the presented model to predict the final orientation of the shear slip lines for the case of non-proportional loading.

Keywords Strain localization, Shear bands, B-bar method, Incompatible modes method

1 Introduction

Ever increasing demand to achieve a more economical structural design requires that a better understanding be obtained of the non-linear behavior of a particular structural system and a reliable estimate be furnished of its limit load. The limit state of a complex system Crisfield 1997a and Crisfield 1997b often implies the presence of particular components whose peak resistance has been already defeated forcing them at that stage to function in post-peak or softening regime.

It is well known by now that the strain-softening phenomena can not reliably be represented by the classical continuum mechanics model, and different remedies leading to a non-standard interpretation of different model ingredients have been proposed: non-local continuum (Bazant et al. 1984), higher order gradient plasticity

(Coleman and Hodgdon 1985), viscoplasticity regularization (Needleman 1988) or Cosserat continuum (De Borst and Sluys 1991), among others. All the modifications of this kind, usually referred to as localization limiters (see Belytschko and Lasry 1989) lead to a significant increase of complexity in formulating the strain localization problems and even more in solving it numerically. For that reason, they seem to be nowadays often replaced by a particular modification of the classical continuum which allows that either displacement or strain discontinuities enter the formulation (Ortiz et al. 1987; Simo et al. 1993; Belytschko et al. 1988; Oliver 1995; Armero and Garikipati 1995; Runesson et al. 1991; Jirasek and Zimmermann 2001 or Qiu et al. 2001 among others). The main advantage of the modified continuum models of this kind is to provide the adequate measure of the total inelastic dissipation of the strain softening component regardless of the chosen finite element mesh, which is the principal information of interest for the limit load computation. However, the vast majority of previous works are typically developed in combination with elastic response, so they can consider only either elastic or strain softening states and thus completely ignore the possible inelastic deformation which can spread outside the strain-softening zone (i.e. the components acting in strain hardening regime).

In this work, we develop a model capable of taking into account both the contribution of a strain hardening as well as a strain softening model component. Such a model is considered to be a more realistic representation of the limit state of a massive structural system where both kind of inelastic dissipations (either strain-hardening or strain-softening) are considered to be non negligible. The model problem considered in detail is the metal plasticity with the von Mises yield criterion governing the strain hardening behavior and shear slip line representing the strain softening behavior. In this case, taking into account the hardening phase will lead in general to stress redistribution and better estimate of shear slip line orientation. It is considered that these two types of behavior are separated by the localization condition, with the strain-hardening behavior appearing as the precursor to shear slip line creation. The crucial condition which allows to connect two states, the states of pre- and post-localization, pertains to imposing the equivalence of the corresponding dissipations, which can be cast as the stress orthogonality with respect to localization induced enhanced strain field. The standard finite element implementation ought to be modified in order to account for this orthogonality condition and addition of corresponding displacement modes

A. Ibrahimbegovic (✉), D. Brancherie
École Normale Supérieure de Cachan,
Laboratoire de Mécanique et Technologie de Cachan 61,
av. du président Wilson 94235 Cachan, France
e-mail: ai@lmt.ens-cachan.fr

Dedicated to the memory of Prof. Mike Crisfield, for his cheerfulness and cooperation as a colleague and friend over many years.

This work was supported by the French Ministry of Research and ACI research program. This support is gratefully acknowledged.

representing displacement discontinuity along yield line, which can be carried out in a very similar manner as for the method of incompatible modes (e.g. Ibrahimbegovic and Wilson 1991). Moreover, in the chosen model problem of von Mises plasticity, a particular choice of the B-bar finite element approximation is also required for the strain hardening phase in order to eliminate potential locking phenomena due to quasi-incompressible behavior (e.g. Nagtegaal et al. 1974 or Hughes 1987). A variational framework which provides the basis for accommodating different strain enhancement in a fully consistent manner is constructed in this work.

The outline of the paper is as follows. In the next section, we lay down the theoretical framework capable of accommodating both strain-hardening and strain-softening effects. For clarity of presentation, we start with 1D case and subsequently extend to more general 2D and 3D cases. Careful considerations of the discrete approximation, based on the finite element method, B-bar and the incompatible mode approximations, are given in Sec. 3. In Sec. 4, we present the results for several illustrative numerical simulations. The concluding remarks are given in Sec. 5.

2

Theoretical formulation

In this section, we develop the governing equations of a boundary value problem where the response can be highly non-homogeneous with one or more sub-domains where the peak stress resistance is reached and which are thus acting in a strain softening regime whereas the rest of the structure still remains placed either in elastic or in elasto-plastic strain hardening regime. The motivation for representing such a combination of plastic zones stems from interpretation of a typical plastic failure pattern of massive structures. The model developed herein for representing this kind of problem is capable of describing both the strain-hardening and strain softening regimes, as well as identifying the stress state which corresponds to passing from hardening to softening. In particular, the latter is considered to coincide with the satisfaction of the localization condition (e.g. Hill 1962 or Rice 1976) modified for the presence of hardening. For clarity of ideas, we first present the development pertinent to 1D case and subsequently generalize to 2D and 3D cases.

2.1

Motivation: hardening/softening plasticity for 1D case

We consider a 1D model for simple shear test, as a bar of length ℓ (of a unit section) built-in at one end and submitted to an imposed shear traction at another end. We limit ourselves to small displacement gradient theory which allows us to keep the standard format of kinematics and equilibrium equations:

$$\bar{\varepsilon} = \frac{\partial \bar{u}}{\partial x} \quad (1)$$

$$\frac{\partial \sigma}{\partial x} + b = 0 \quad (2)$$

where \bar{u} , $\bar{\varepsilon}$ and σ are, respectively, transverse displacement, infinitesimal deformation and the Cauchy stress field,

whereas b is the external distributed loading. In (1) above all the fields with superposed bar are considered as smooth, which tacitly implies hardening plasticity. If the external loading in (2) is equal to zero, it can be concluded that the stress σ will also be smooth (constant) along the bar.

The constitutive model of plasticity can be constructed starting with those essential ingredients:

- additive decomposition of total strain into elastic $\bar{\varepsilon}^e$ and plastic component $\bar{\varepsilon}^p$

$$\bar{\varepsilon} = \bar{\varepsilon}^e + \bar{\varepsilon}^p \quad (3)$$

- strain energy function depending upon elastic strain and hardening variable $\bar{\xi}$

$$\bar{\psi}(\bar{\varepsilon}^e, \bar{\xi}) = \frac{1}{2} \bar{\varepsilon}^e E \bar{\varepsilon}^e + \bar{\Xi}(\bar{\xi}) \quad (4)$$

and

- the yield criterion specifying the admissible values of stress and stress-like hardening variable \bar{q}

$$\bar{\phi}(\sigma, \bar{q}) = |\sigma| - (\sigma_y - \bar{q}) \leq 0 \quad (5)$$

where σ_y denotes the yield stress.

All the remaining ingredients of the plasticity model can be obtained from the standard thermodynamics considerations and the principle of the maximum plastic dissipation (Lubliner 1990). Namely, the second law of thermodynamics (Truesdell and Noll 1965; Lubliner 1990 or Maugin 1992) states that the dissipation always remains non-negative, which can be written by making use of the results (3) and (4) as:

$$\begin{aligned} 0 \leq \mathcal{D} &= \sigma \dot{\bar{\varepsilon}} - \frac{d}{dt} \bar{\psi}(\bar{\varepsilon}^e, \bar{\xi}) \\ &= \left(\sigma - \frac{\partial \bar{\psi}}{\partial \bar{\varepsilon}^e} \right) \dot{\bar{\varepsilon}}^e + \frac{\partial \bar{\psi}}{\partial \bar{\varepsilon}^e} \dot{\bar{\varepsilon}}^p - \frac{\partial \bar{\Xi}}{\partial \bar{\xi}} \dot{\bar{\xi}} \end{aligned} \quad (6)$$

One can conclude from the last equation that in an elastic process, with no change of internal variables ($\dot{\bar{\varepsilon}}^p = 0$, $\dot{\bar{\xi}} = 0$) and no dissipation, the stress like variables can be defined through the following constitutive equations:

$$\begin{aligned} \bar{\phi} < 0, \quad \dot{\bar{\varepsilon}}^p = 0, \quad \dot{\bar{\xi}} = 0, \\ \mathcal{D} = 0 \implies \sigma = \frac{\partial \bar{\psi}}{\partial \bar{\varepsilon}^e}; \quad \bar{q} = - \frac{\partial \bar{\Xi}}{\partial \bar{\xi}} \end{aligned} \quad (7)$$

Assuming that the constitutive equations in (7) remain valid in a plastic process, one can define the (positive) plastic dissipation as:

$$\bar{\phi} = 0; \quad 0 < \mathcal{D}^p = \sigma \dot{\bar{\varepsilon}}^p + \bar{q} \dot{\bar{\xi}} \quad (8)$$

The evolution equations of internal variables for such a process can be obtained by appealing to the principle of maximum plastic dissipation; which states that among all admissible values of stress satisfying (5), we ought to select those which maximize the plastic dissipation, or otherwise:

$$(\sigma, \bar{q}) = \arg \left\{ \min_{\bar{\phi}(\sigma^*, \bar{q}^*)} [-\mathcal{D}^p(\sigma^*, \bar{q}^*)] \right\} \quad (9)$$

The same problem can be recast as a minimization problem with constraint by appealing to the Lagrange multiplier method and introducing the Lagrangian

$$\max_{\forall \dot{\gamma} > 0} \min_{\forall (\sigma^*, \bar{q}^*, \dot{\gamma})} \mathcal{L}^P(\sigma^*, \bar{q}^*, \dot{\gamma}); \quad \mathcal{L}^P(\cdot) = -\mathcal{D}^P(\cdot) + \dot{\gamma} \bar{\phi}(\cdot) \quad (10)$$

The Kuhn–Tucker optimality conditions (see Luenberger 1984 or Strang 1986) of this problem can readily be obtained leading to the evolution equation of the internal variables.

$$\begin{aligned} \frac{\partial \mathcal{L}^P}{\partial \sigma} = 0 &\Rightarrow \dot{\varepsilon}^p = \dot{\gamma} \frac{\partial \bar{\phi}}{\partial \sigma} = \dot{\sigma} \text{sign}(\sigma) \\ \frac{\partial \mathcal{L}^P}{\partial \bar{q}} = 0 &\Rightarrow \dot{\xi} = \dot{\gamma} \frac{\partial \bar{\phi}}{\partial \bar{q}} = \dot{\gamma} \end{aligned} \quad (11)$$

We also obtain the constraint equation which can be combined with the corresponding value in (8) for the elastic case to provide the final form of the loading/unloading conditions:

$$\dot{\gamma} \geq 0, \quad \bar{\phi} \leq 0 \Rightarrow \dot{\gamma} \bar{\phi} = 0 \quad (12)$$

The only case of plastic loading which gives a non-zero value of $\dot{\gamma}$ can be developed further by appealing to the consistency condition to guarantee the admissibility of stress for subsequent states:

$$\begin{aligned} \dot{\sigma} &= E \left(\dot{\varepsilon}^e - \underbrace{\dot{\gamma} \frac{\partial \bar{\phi}}{\partial \sigma}}_{\dot{\varepsilon}^p} \right) \\ \dot{\bar{q}} &= - \underbrace{\frac{d^2 \bar{\Xi}}{d \bar{\xi}^2}}_{\bar{K}} \underbrace{\dot{\xi}}_{\dot{\gamma} \frac{\partial \bar{\phi}}{\partial \bar{q}}} \\ 0 &= \frac{d}{dt} \bar{\phi} = \frac{\partial \bar{\phi}}{\partial \sigma} \dot{\sigma} + \frac{\partial \bar{\phi}}{\partial \bar{q}} \dot{\bar{q}} \\ &= \frac{\partial \bar{\phi}}{\partial \sigma} E \dot{\varepsilon} - \dot{\gamma} \left(\frac{\partial \bar{\phi}}{\partial \sigma} E \frac{\partial \bar{\phi}}{\partial \sigma} + \frac{\partial \bar{\phi}}{\partial \bar{q}} \bar{K} \frac{\partial \bar{\phi}}{\partial \bar{q}} \right) \\ &\Rightarrow \dot{\gamma} = \frac{\frac{\partial \bar{\phi}}{\partial \sigma} E \dot{\varepsilon}}{\frac{\partial \bar{\phi}}{\partial \sigma} E \frac{\partial \bar{\phi}}{\partial \sigma} + \frac{\partial \bar{\phi}}{\partial \bar{q}} \bar{K} \frac{\partial \bar{\phi}}{\partial \bar{q}}} \end{aligned} \quad (13)$$

with this result in hands, we can further provide the rate form of the stress–strain constitutive equations according to:

$$\dot{\sigma} = \begin{cases} E \dot{\varepsilon} & \dot{\gamma} = 0 \\ \left[E - \frac{E \frac{\partial \bar{\phi}}{\partial \sigma} E \frac{\partial \bar{\phi}}{\partial \sigma}}{\frac{\partial \bar{\phi}}{\partial \sigma} E \frac{\partial \bar{\phi}}{\partial \sigma} + \frac{\partial \bar{\phi}}{\partial \bar{q}} \bar{K} \frac{\partial \bar{\phi}}{\partial \bar{q}}} \right] \dot{\varepsilon} & \dot{\gamma} > 0 \end{cases} \quad (14)$$

In particular, for the yield criterion in (5), leading to $\partial \bar{\phi} / \partial \sigma = \text{sign}(\sigma)$ and $\partial \bar{\phi} / \partial \bar{q} = 1$, we can further obtain a simplified form of the stress rate equation for plastic loading as:

$$\dot{\sigma} = \frac{E \bar{K}}{E + \bar{K}} \dot{\varepsilon} \quad \dot{\gamma} > 0 \quad (15)$$

We can see that the stress will keep increasing with increasing values of strains only as long as we remain in strain hardening regime with $\bar{K} = (d^2 \bar{\Xi} / d \bar{\xi}^2) > 0$. The peak resistance in the stress–strain diagram is identified at :

$$C^{\text{ep}} = \frac{E \bar{K}}{E + \bar{K}} = 0 \Rightarrow \bar{K} = \frac{d^2 \bar{\Xi}}{d \bar{\xi}^2} = 0 \quad (16)$$

We assume that $\bar{K}(\bar{\xi}_u) = 0$, and that $\sigma_u = \sigma_y - \bar{q}(\bar{\xi}_u)$ is the ultimate value of stress. Supposing we then enter the softening phase, with $\bar{K} < 0$, according to (15) the increase in strain will lead to the decrease in stress. Such a case is fundamentally different from the strain hardening case as shown by the following analysis. Namely, in the latter case 1D problem under consideration with zero external load and constant stress state will lead to gradual spreading of the plasticity throughout the domain, starting from the first plastified section, since the stress will keep increasing. For the same constant stress state and strain-softening case, the first section which passes the peak (typically a slightly weakened section which is supposed to transform a bifurcation into a limit load problem) will reduce the stress level leading to unloading in all other sections where peak is not passed; all subsequent inelastic deformation will be accumulated in the particular section where the shear band is created. Considering that the shear band thickness tends to zero, we can assume that the displacement field can be written as:

$$u(x, t) = \bar{u}(x, t) + \bar{\eta}(t) M_{\bar{x}}(x) \quad (17)$$

with

$$\begin{aligned} M_{\bar{x}}(x) &= H_{\bar{x}}(x) - N_a(x); \\ H_{\bar{x}}(x) &= \begin{cases} 1, & x > \bar{x} \\ 0, & x < \bar{x} \end{cases}; \\ N_a(x) &= \begin{cases} 1, & x = l \\ 0, & x = 0 \end{cases} \end{aligned} \quad (18)$$

In (17) above $\bar{u}(x, t)$ is the smooth displacement field, and $\bar{\eta}(t)$ is the displacement discontinuity which appears at the shear band location \bar{x} .

By differentiating this expression we obtain the corresponding strain field which contains a regular (smooth) $\bar{\varepsilon}$ and singular components:

$$\varepsilon(x, t) = \underbrace{\bar{\varepsilon}(x, t)}_{\bar{\varepsilon}} + \bar{\eta}(t) G(x) + \bar{\eta}(t) \delta_{\bar{x}}(x) \quad (19)$$

where $\delta_{\bar{x}}(x)$ denotes Dirac delta function at point \bar{x} .

In accordance with this new form of the strain field, the strain energy can also be split into a regular and a singular part as:

$$\psi(\varepsilon, \bar{\xi}, \bar{\xi}) = \bar{\psi}(\bar{\varepsilon}^e, \bar{\xi}) + \bar{\psi}(\bar{\xi}) \delta_{\bar{x}}(x) \quad (20)$$

where $\bar{\xi}$ is the internal variable which describes the softening phenomena on discontinuity.

The dissipation inequality can be written by making use of the result in (20) leading to

$$\begin{aligned} 0 &\leq \mathcal{D}_{\Omega}^{\text{loc}} = \int_{\Omega} \left[\sigma \dot{\varepsilon} - \frac{d}{dt} \psi(\varepsilon, \bar{\xi}, \bar{\xi}) \right] dx \\ &= \int_{\Omega} \left[\sigma \dot{\varepsilon} - \frac{d}{dt} \bar{\psi}(\bar{\varepsilon}^e, \bar{\xi}) \right] dx + \left[t \dot{\bar{\eta}} - \frac{d}{dt} \bar{\psi}(\bar{\xi}) \right]_{\bar{x}} \end{aligned} \quad (21)$$

where we used the definition of Dirac delta function in (19) to obtain the traction at discontinuity as:

$$t = \sigma|_{\bar{x}} \quad (22)$$

Comparing the last expression with the one in (8), we can conclude that the dissipation in post-localization phase can be reduced to the sum of the regular and singular components which can be written as:

$$\mathcal{D}_{\Omega}^{\text{loc}} = \int_{\Omega} \underbrace{\sigma \dot{\varepsilon}^{\text{p}} + q \dot{\xi}}_{\mathcal{D}_{\Omega}} dx + [\bar{q}\bar{\xi}]|_{\bar{x}}; \quad \bar{q} = -\frac{\partial \bar{\psi}}{\partial \bar{\xi}} \quad (23)$$

if the following condition applies

$$\int_{\Omega} G(x)\sigma dx + t = 0 \quad (24)$$

The expression in (24) above is considered as an orthogonality condition which ought to be imposed and solved for simultaneously with the global equilibrium equations.

The second term in (21) above represents the contribution of the discontinuity to the total dissipation. In order to develop further the exact nature of such a contribution, we postulate the yield criterion at discontinuity which defines the corresponding admissible traction values according to

$$\bar{\phi}(t, \bar{q}) := |t| - (\sigma_u - \bar{q}) = 0 \quad (25)$$

The principle of maximum plastic dissipation applied to the case where only discontinuity remains active can be written by introducing the Lagrange multiplier in the form:

$$\gamma = \bar{\gamma} \delta_{\bar{x}} \quad (26)$$

which further restricts the corresponding Lagrangian to the discontinuity according to:

$$\begin{aligned} \mathcal{L}^{\text{p}}(\bar{q}, \bar{\gamma}) &= \left[-\bar{q}\bar{\xi} \right]_{\bar{x}} + \int_{\Omega} \underbrace{\bar{\gamma} \delta_{\bar{x}}}_{\dot{\gamma}} \bar{\phi} dx \\ &= \left[-\bar{q}\bar{\xi} + \bar{\gamma}\bar{\phi} \right]_{\bar{x}} \end{aligned} \quad (27)$$

The Kuhn-Tucker optimality conditions then reduce to:

$$\begin{aligned} \dot{\bar{\xi}} &= \dot{\bar{\gamma}} \\ \dot{\bar{\gamma}} &\geq 0, \quad \bar{\phi} \leq 0, \quad \bar{\gamma}\bar{\phi} = 0 \end{aligned} \quad (28)$$

The time derivative of this yield criterion furnishes the consistency condition to compute the corresponding value of the plastic multiplier with:

$$0 = \text{sign}(t)\dot{t} + \underbrace{\frac{\partial \bar{q}}{\partial \bar{\xi}}}_{-\bar{K}} \dot{\bar{\xi}} \Rightarrow \dot{\bar{\gamma}} = \frac{1}{\bar{K}} \dot{t} \text{sign}(t) \quad (29)$$

where the result in (28) above was exploited. It is important to note that the rate of change of traction at discontinuity can not be computed from a constitutive equation; it is rather obtained from the time derivative of the orthogonality condition in (23), leading to

$$\dot{\bar{\gamma}} = \frac{1}{\bar{K}} \int_{\Omega} G \dot{\sigma} dx \quad (30)$$

The rigid-plastic traction displacement law employed in this work implies that the presence of discontinuity does not affect at all the elastic response. The corresponding coefficients of the traction displacement law to be chosen are: traction yield value $t_y = \sigma_u$, which is chosen in accordance with the ultimate values of stress in the hardening regime, and the softening modulus which depends on a particular choice of softening law.

Let us denote as G_f the total external work expended in the process of driving the effective flow traction $t_y^{\text{eff}} = t_y - \bar{q}$, to zero. Assuming linear softening law we can thus obtain the corresponding value of the softening modulus \bar{K} from the following condition:

$$\begin{aligned} 0 &= t_y - |\bar{K}| \bar{\xi}_u \Rightarrow \bar{\xi}_u = \frac{t_y}{|\bar{K}|} \\ G_f &= \frac{1}{2} t_y \bar{\xi}_u = \frac{1}{2} \frac{t_y^2}{|\bar{K}|} \Rightarrow \bar{K} = -\frac{1}{2} \frac{t_y^2}{G_f} \end{aligned} \quad (31)$$

One can easily modify linear softening law in (31). For example, with an exponential softening response we can write:

$$\begin{aligned} G_f &= \int_0^{\infty} t_y \exp(-\alpha \bar{\xi}) d\bar{\xi} = -\frac{t_y}{\alpha} [\exp(-\alpha \bar{\xi})]_0^{\infty} \Rightarrow t_y - \bar{q}(\bar{\xi}) \\ &= t_y \exp\left(-\frac{t_y}{G_f} \bar{\xi}\right) \end{aligned} \quad (32)$$

2.2

Extension to 2D/3D case

In this section, we seek to extend the validity of the presented 1D model to a general 2D/3D case. Moreover, by making particular choice of the von Mises yield criterion, we set to develop a suitable approach to treat the precursor to failure in terms of the well-known shear band softening response. The basic ideas already introduced in the 1D framework remain unaffected, and the main novelty is brought about by the tensor notion needed to describe this 2D/3D case. In particular, the two sets of equations, describing the kinematics and equilibrium now can be written as:

$$\begin{aligned} \bar{\varepsilon} &= \mathbf{V}^s \bar{\mathbf{u}} \\ \text{div}[\bar{\sigma}] + \mathbf{b} &= 0 \end{aligned} \quad (33)$$

where $\mathbf{V}^s(\cdot)$ denotes the symmetric part of the gradient and $\text{div}(\cdot)$ the divergence operator. Starting again with the hardening case where the strain and displacement fields remain smooth as indicated with a superposed bar in (33) above, by analogy with (3) to (5) we can write the three main ingredients of the constitutive model as:

- additive decomposition of the total strain into its elastic and inelastic components

$$\bar{\boldsymbol{\varepsilon}} = \bar{\boldsymbol{\varepsilon}}^e + \bar{\boldsymbol{\varepsilon}}^p \quad (34)$$

- the strain energy

$$\bar{\psi}(\bar{\boldsymbol{\varepsilon}}^e, \bar{\xi}) = \frac{1}{2} \bar{\boldsymbol{\varepsilon}}^e \cdot \mathbf{C} \bar{\boldsymbol{\varepsilon}}^e + \bar{\Xi}(\bar{\xi}) \quad (35)$$

- and the yield criterion of von Mises

$$\bar{\phi}(\boldsymbol{\sigma}, \bar{q}) = \sqrt{\frac{3}{2}} \|\text{dev}[\boldsymbol{\sigma}]\| - (\sigma_y - \bar{q}) \quad (36)$$

where $\text{dev}[\boldsymbol{\sigma}] = \boldsymbol{\sigma} - \frac{1}{3} \text{tr}(\boldsymbol{\sigma}) \mathbf{1}$ is the deviator part of the stress tensor.

The remaining ingredients of the model can again be obtained by appealing to the second principle of thermodynamics:

$$\begin{aligned} 0 \leq \mathcal{D} &= \boldsymbol{\sigma} \cdot \dot{\bar{\boldsymbol{\varepsilon}}} - \frac{d}{dt} \bar{\psi}(\bar{\boldsymbol{\varepsilon}}, \bar{\xi}) \\ &= \left(\boldsymbol{\sigma} - \frac{\partial \bar{\psi}}{\partial \bar{\boldsymbol{\varepsilon}}^e} \right) \cdot \dot{\bar{\boldsymbol{\varepsilon}}} + \boldsymbol{\sigma} \cdot \dot{\bar{\boldsymbol{\varepsilon}}^p} + \bar{q} \dot{\bar{\xi}} \end{aligned} \quad (37)$$

which gives the stress constitutive equations and defines the plastic dissipation:

$$\boldsymbol{\sigma} = \frac{\partial \bar{\psi}}{\partial \bar{\boldsymbol{\varepsilon}}^e} = \mathbf{C}(\bar{\boldsymbol{\varepsilon}} - \bar{\boldsymbol{\varepsilon}}^p) \quad (38)$$

$$0 < \mathcal{D} = \boldsymbol{\sigma} \cdot \dot{\bar{\boldsymbol{\varepsilon}}^p} + \bar{q} \dot{\bar{\xi}}$$

The principle of the maximum plastic dissipation is then used to obtain the evolution equations for the internal variables with:

$$\max_{\forall \dot{\gamma} > 0} \min_{\forall (\boldsymbol{\sigma}^*, \bar{q}^*, \dot{\gamma}^*)} \mathcal{L}^p(\boldsymbol{\sigma}^*, \bar{q}^*, \dot{\gamma}^*);$$

$$\mathcal{L}^p(\cdot) = -\mathcal{D}^p(\cdot) + \dot{\gamma} \bar{\phi}(\cdot) \quad (39)$$

$$\frac{\partial \mathcal{L}^p}{\partial \boldsymbol{\sigma}} = 0 \Rightarrow \dot{\bar{\boldsymbol{\varepsilon}}^p} = \dot{\gamma} \frac{\partial \bar{\phi}}{\partial \boldsymbol{\sigma}} = \dot{\gamma} \frac{\text{dev}[\boldsymbol{\sigma}]}{\|\text{dev}[\boldsymbol{\sigma}]\|} \sqrt{\frac{3}{2}} \quad (40)$$

$$\frac{\partial \mathcal{L}^p}{\partial \bar{q}} = 0 \Rightarrow \dot{\bar{\xi}} = \dot{\gamma} \frac{\partial \bar{\phi}}{\partial \bar{q}} = \dot{\gamma}$$

The last result implies that the plastic deformation remains purely deviatoric. By admitting that plastic multiplier can take both positive and zero value, we can write the loading/unloading conditions according to:

$$\dot{\gamma} \geq 0, \quad \bar{\phi} \leq 0, \quad \dot{\gamma} \bar{\phi} = 0 \quad (41)$$

with the key property of the von Mises yield function $\frac{\partial \bar{\phi}}{\partial \boldsymbol{\sigma}} \cdot \boldsymbol{\sigma} = \dot{\phi}$. The only non-zero value of the plastic multiplier is obtained for plastic loading case from the local form of the consistency conditions according to:

$$\begin{aligned} 0 = \dot{\phi} &= \frac{\partial \bar{\phi}}{\partial \boldsymbol{\sigma}} \cdot \dot{\boldsymbol{\sigma}} + \frac{\partial \bar{\phi}}{\partial \bar{q}} \cdot \dot{\bar{q}} \\ &= \frac{\partial \bar{\phi}}{\partial \boldsymbol{\sigma}} \cdot \mathbf{C} \dot{\bar{\boldsymbol{\varepsilon}}} - \dot{\gamma} \left(\frac{\partial \bar{\phi}}{\partial \boldsymbol{\sigma}} \cdot \mathbf{C} \frac{\partial \bar{\phi}}{\partial \boldsymbol{\sigma}} + \frac{\partial \bar{\phi}}{\partial \bar{q}} \bar{K} \frac{\partial \bar{\phi}}{\partial \bar{q}} \right) \end{aligned} \quad (42)$$

$$\dot{\gamma} = \frac{\frac{\partial \bar{\phi}}{\partial \boldsymbol{\sigma}} \cdot \mathbf{C} \dot{\bar{\boldsymbol{\varepsilon}}}}{\frac{\partial \bar{\phi}}{\partial \boldsymbol{\sigma}} \cdot \mathbf{C} \frac{\partial \bar{\phi}}{\partial \boldsymbol{\sigma}} + \frac{\partial \bar{\phi}}{\partial \bar{q}} \bar{K} \frac{\partial \bar{\phi}}{\partial \bar{q}}} = \frac{\sqrt{6} \mu}{(3\mu + \bar{K}) \|\mathbf{s}\|} \mathbf{s}, \quad \mathbf{s} = \text{dev}[\boldsymbol{\sigma}]$$

which allows to write the rate form of the stress constitutive equation according to:

$$\begin{aligned} \dot{\boldsymbol{\sigma}} &= \mathbf{C}^{\text{ep}} \dot{\bar{\boldsymbol{\varepsilon}}} \\ \mathbf{C}^{\text{ep}} &= \begin{cases} \mathbf{C}; & \dot{\gamma} = 0 \\ \mathbf{C} - \frac{1}{\frac{\partial \bar{\phi}}{\partial \boldsymbol{\sigma}} \cdot \mathbf{C} \frac{\partial \bar{\phi}}{\partial \boldsymbol{\sigma}} + \frac{\partial \bar{\phi}}{\partial \bar{q}} \bar{K} \frac{\partial \bar{\phi}}{\partial \bar{q}}} \mathbf{C} \frac{\partial \bar{\phi}}{\partial \boldsymbol{\sigma}} \otimes \mathbf{C} \frac{\partial \bar{\phi}}{\partial \boldsymbol{\sigma}} & \dot{\gamma} > 0 \\ = \mathbf{C} - \frac{2\mu}{(1 + \frac{\bar{K}}{3\mu}) \|\mathbf{s}\|^2} \mathbf{s} \otimes \mathbf{s}; & \dot{\gamma} > 0 \end{cases} \end{aligned} \quad (43)$$

In extending this model to softening phase we assume that the slip line creation will mark the softening phase. The displacement field in the presence of the slip line no longer remains smooth and one should take into account the displacement jump analogous to the one in (17) from 1D case.

If we denote by Γ_s the displacement discontinuity line separating the domain in two subdomains, Ω^+ and Ω^- (see Fig. 1)

$$\mathbf{u}(\mathbf{x}, t) = \bar{\mathbf{u}}(t) + \bar{\boldsymbol{\eta}}(\mathbf{x}, t) M_{\Gamma_s}(\mathbf{x})$$

$$M_{\Gamma_s}(\mathbf{x}) = H_{\Gamma_s}(\mathbf{x}) - N(\mathbf{x}); \quad H_{\Gamma_s}(\mathbf{x}) = \begin{cases} 1, & \mathbf{x} \in \Omega^+ \\ 0, & \mathbf{x} \in \Omega^- \end{cases} \quad (44)$$

where $\bar{\boldsymbol{\eta}}(t)$ represents the amplitude of the displacement jump along Γ_s . Assuming that the latter will increase in time always remaining of constant direction along the discontinuity leads to:

$$\dot{\bar{\boldsymbol{\eta}}}(t) = \dot{\eta}(t) \mathbf{m}; \quad \dot{\eta}(t)|_{\Gamma_s} = \text{cst} \quad (45)$$

where \mathbf{m} is the unit vector tangent to the slip line.

The result in (45) further implies that directional derivative of displacement along discontinuity must remain zero:

$$0 = \mathbf{D}_\ell \dot{\bar{\boldsymbol{\eta}}}(\mathbf{x}, t) = \nabla \dot{\bar{\boldsymbol{\eta}}} \mathbf{m} \, ds; \quad \mathbf{m}^T \mathbf{n} = 0 \quad (46)$$

where \mathbf{n} is the unit normal vector on Γ_s (see Fig. 1). By comparing (45) and (46) we can conclude that it must hold that:

$$\nabla \dot{\bar{\boldsymbol{\eta}}} = \dot{\eta} \mathbf{m} \otimes \mathbf{n} \quad (47)$$

In the spirit of the classical works on localization problems (Hill 1962; Mandel 1966 or Rice 1976), we assume that the bifurcation phenomena in an elasto-plastic response can be interpolated as the difference between two smooth stress fields, defining the corresponding jump in the stress rate as:

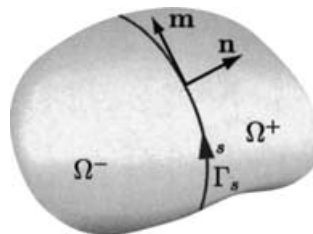


Fig. 1. Slip line Γ_s separating the domain into Ω^+ and Ω^-

$$\llbracket \dot{\boldsymbol{\sigma}} \rrbracket = \mathbf{C}^{\text{ep}}(\mathbf{m} \otimes \dot{\mathbf{n}}\bar{\eta}) \quad (48)$$

Furthermore, according to the Newton third law which imposes the continuity of traction across displacement discontinuity line Γ_s and the Cauchy principle which relates the traction vector to stress tensor, we can write:

$$\mathbf{0} = \llbracket \mathbf{t} \rrbracket = \llbracket \boldsymbol{\sigma} \rrbracket \mathbf{n} + \llbracket \boldsymbol{\sigma} \rrbracket \underbrace{\dot{\mathbf{n}}}_{=0} \quad (49)$$

where the second term drops out because it is assumed that the direction of the discontinuity remains fixed in time. By combining the last two results, we obtain:

$$\begin{aligned} \mathbf{0} &= \mathbf{C}^{\text{ep}}(\mathbf{m} \otimes \dot{\mathbf{n}}\bar{\eta})\mathbf{n} \\ &= \dot{\bar{\eta}}\mathbf{A}^{\text{ep}}\mathbf{m} \end{aligned} \quad (50)$$

where \mathbf{A}^{ep} is the acoustic tensor. For the case under consideration which remains compatible with the von Mises yield criterion, where the plastic deformation in the softening phase remains incompressible as indicated in (46), the acoustic tensor can be rewritten as:

$$\mathbf{A}^{\text{ep}} = \mu \mathbf{1} - \frac{2\mu}{(1 + \frac{\bar{K}}{3\mu})\|\mathbf{s}\|^2} \mathbf{sn} \otimes \mathbf{sn} \quad (51)$$

where μ and \bar{K} are, respectively, shear and hardening moduli.

Computing the principal values of the acoustic tensor, one arrives at the characteristic equation which can be written in the reference system of principal values of stress:

$$\begin{aligned} 0 &= \det[\mathbf{A}^{\text{ep}} - \lambda \mathbf{1}] = (\lambda^* - 1)^2 \left\{ \frac{2}{(1 + \frac{\bar{K}}{3\mu})\|\mathbf{s}\|^2} \right. \\ &\quad \left. \times (n_1^2 s_1^2 + n_2^2 s_2^2) + \lambda^* - 1 \right\}; \quad \lambda^* = \frac{\lambda}{\mu} \end{aligned} \quad (52)$$

By imposing the localization condition in (50) with $\lambda_1^* = 0$, we obtain from (52) above that

$$\bar{K} = 3\mu \left[\left(\frac{\sqrt{2}\tau}{\|\mathbf{s}\|} \sin 2\theta \right)^2 - 1 \right]; \quad \tau = \frac{1}{2}(\sigma_1 - \sigma_2) \quad (53)$$

By further assuming that the localization condition occurs at the peak resistance where $\bar{K}(\bar{\xi}_u) = 0$, we can obtain that the slip line is formed at the angle θ defined with

$$\theta = \frac{1}{2} \sin^{-1} \left(\frac{\|\mathbf{s}\|}{\sqrt{2}\tau} \right) \quad (54)$$

By computing the value of $\|\mathbf{s}\|$ in terms of principal value stress, we can further obtain that

$$1 = \left(\frac{\sqrt{2}\tau}{\|\mathbf{s}\|/\sqrt{2}} \right)^2 + \left(\frac{p + 3B\varepsilon_{33}^p}{\|\mathbf{s}\|/\sqrt{2}} \right)^2 \frac{(1-2\nu)^2}{3}; \quad (55)$$

$$B = \frac{E}{3(1-2\nu)}; \quad p = \frac{\text{tr}[\boldsymbol{\sigma}]}{3}$$

It then follows from (54) and (55) that for the case of (quasi-) incompressible material, or when the pressure p is

related to $3B\varepsilon_{33}^p$, the slip line will occur at 45° with respect to the maximum principal stress.

Having established that the localization condition coincides with the initiation of the displacement discontinuity, we turn to the final phase of the analysis where the discontinuity remains active. The strain field in this case is written as:

$$\boldsymbol{\varepsilon} = \nabla^s \mathbf{u} = \nabla^s \bar{\mathbf{u}} + \underbrace{\tilde{\mathbf{G}}\bar{\boldsymbol{\eta}}}_{\bar{\boldsymbol{\varepsilon}}} + \bar{\boldsymbol{\eta}}(\mathbf{m} \otimes \mathbf{n})^s \delta_{\Gamma_s} \quad (56)$$

such that

$$\int_{\Omega} \tilde{\mathbf{G}} \, d\Omega + \int_{\Gamma_s} (\mathbf{m} \otimes \mathbf{n})^s \, d\Gamma_s = \mathbf{0} \quad (57)$$

In (57) above we used the results in (45) and the well-known result in distribution theory, (e.g. see Stakgold 1979) that

$$\int_{\Omega} \phi \nabla H_{\Gamma_s} \, d\Omega = \int_{\Gamma_s} \phi \mathbf{n} \, d\Gamma_s \quad (58)$$

In accordance with such a form of the strain field, we split the strain energy by separating the smooth part from the discontinuity contribution:

$$\psi(\boldsymbol{\varepsilon}, \bar{\boldsymbol{\xi}}, \bar{\boldsymbol{\xi}}) = \bar{\psi}(\bar{\boldsymbol{\varepsilon}}^e, \bar{\boldsymbol{\xi}}) + \bar{\psi}(\bar{\boldsymbol{\xi}}) \delta_{\Gamma_s} \quad (59)$$

The dissipation inequality can thus be written as:

$$\begin{aligned} 0 &\leq \mathcal{D}_{\Omega}^{\text{loc}} = \int_{\Omega} \left[\boldsymbol{\sigma} \cdot \dot{\boldsymbol{\varepsilon}} - \frac{d}{dt} \psi(\boldsymbol{\varepsilon}, \bar{\boldsymbol{\xi}}, \bar{\boldsymbol{\xi}}) \right] d\Omega \\ &= \int_{\Omega} \left[\boldsymbol{\sigma} \cdot \dot{\bar{\boldsymbol{\varepsilon}}} - \frac{d}{dt} \bar{\psi}(\bar{\boldsymbol{\varepsilon}}^e, \bar{\boldsymbol{\xi}}) \right] d\Omega \\ &\quad + \int_{\Gamma_s} [\mathbf{t} \cdot \dot{\bar{\boldsymbol{\eta}}}] ds - \int_{\Gamma_s} \left[\frac{d}{dt} \bar{\psi}(\bar{\boldsymbol{\xi}}) \right] ds \end{aligned} \quad (60)$$

If we further assume that the following stress orthogonality condition must be satisfied:

$$\int_{\Omega} \boldsymbol{\sigma} \cdot \tilde{\mathbf{G}}\dot{\bar{\boldsymbol{\eta}}} \, d\Omega + \int_{\Gamma_s} \mathbf{t} \cdot \dot{\bar{\boldsymbol{\eta}}} \, ds = 0 \quad (61)$$

We recover from (60) above the stress constitutive equation from (38) and the total dissipation reduced to the sum of two parts, in volume and slip line:

$$\mathcal{D}_{\Omega}^{\text{loc}} = \underbrace{\int_{\Omega} \boldsymbol{\sigma} \cdot \dot{\bar{\boldsymbol{\varepsilon}}}^p + \bar{q}\dot{\bar{\boldsymbol{\xi}}} \, d\Omega}_{\mathcal{D}_{\Omega}^p} + \underbrace{\int_{\Gamma_s} \bar{q} \cdot \dot{\bar{\boldsymbol{\xi}}} \, ds}_{\mathcal{D}_{\Gamma_s}^p} \quad (62)$$

Once the localized solution develops, the stress orthogonality condition in (61) should be joined and solved along the set of global equilibrium equations. The yield condition controlling inelastic deformation at discontinuity is set directly in terms of the traction vector component $t_m = \mathbf{t} \cdot \mathbf{m}$:

$$\bar{\phi}(\mathbf{t}, \bar{\mathbf{q}}) = |t_m| - (t_y - \bar{\mathbf{q}}) \leq 0 \quad (63)$$

Assuming further that the plastic multiplier takes the form $\dot{\gamma} = \dot{\bar{\gamma}} + \dot{\bar{\gamma}}\delta_{\Gamma_s}$, we can make use of the principle of maximum plastic dissipation with:

$$\begin{aligned} \max_{\forall \bar{\gamma} > 0} \min_{\forall (\mathbf{t}^*, \bar{\mathbf{q}}^*)} \bar{\mathcal{L}}^P(\boldsymbol{\sigma}^*, \bar{\mathbf{q}}^*, \dot{\bar{\gamma}}); \quad \bar{\mathcal{L}}^P(\cdot) \\ = -\mathcal{D}_{\Omega}^{\text{loc}}(\cdot) + \int_{\Omega} \dot{\bar{\gamma}} \bar{\phi} d\Omega + \int_{\Gamma_s} \dot{\bar{\gamma}} \bar{\phi}(\cdot) ds \end{aligned} \quad (64)$$

The corresponding Kuhn–Tucker optimality conditions can then be written as:

$$\begin{aligned} 0 &= \int_{\Omega} \left(-\dot{\bar{\boldsymbol{\varepsilon}}}^P + \dot{\bar{\gamma}} \frac{\partial \bar{\phi}}{\partial \boldsymbol{\sigma}} \right) d\Omega \\ 0 &= \int_{\Omega} \left(-\dot{\bar{\boldsymbol{\xi}}} + \dot{\bar{\gamma}} \frac{\partial \bar{\phi}}{\partial \bar{\mathbf{q}}} \right) d\Omega \end{aligned} \quad (65)$$

accompanied with

$$0 = \int_{\Gamma_s} \left(-\dot{\bar{\boldsymbol{\xi}}} + \dot{\bar{\gamma}} \frac{\partial \bar{\phi}}{\partial \bar{\mathbf{q}}} \right) ds \Rightarrow \int_{\Gamma_s} \dot{\bar{\boldsymbol{\xi}}} ds = \int_{\Gamma_s} \dot{\bar{\gamma}} ds \quad (66)$$

In closing this section we note that the combination of two kinds of dissipation is thus essentially handled by the corresponding value of the plastic multiplier. Namely, for the plastic loading case, it is either $\dot{\bar{\gamma}}$ or $\dot{\bar{\boldsymbol{\xi}}}$ or both which remain positive.

The corresponding value of the latter is obtained from the time derivative of (63) by exploiting the results in (61) and (65) to get

$$\dot{\bar{\boldsymbol{\xi}}} = \frac{1}{\bar{\mathbf{K}}} \int_{\Omega} \tilde{\mathbf{G}} \dot{\boldsymbol{\sigma}} d\Omega \quad (67)$$

If the localization condition in (50) is reached within a given time increment, one can then separate the step in one part where $\dot{\bar{\boldsymbol{\xi}}}$ evolves and the remaining part where only $\dot{\bar{\gamma}}$ will be modified computing the corresponding dissipation as indicated in (67). One can also compute the corresponding ‘‘ultimate’’ value of hardening variable $\bar{\boldsymbol{\xi}}_u$ occurring in such a time step.

3 Finite element implementation: mixed-enhanced quadrilateral element

The finite element based discrete approximation (Hughes 1987; Bathe 1996; or Zienkiewicz and Taylor 2000) of the problem on hand can be used to transform the weak form of differential equilibrium equation in (33) into a set of algebraic equations with nodal values of displacements as unknowns:

$$\begin{aligned} \text{Nel} \\ \mathbf{A} \left[\mathbf{f}^{\text{int},e}(t) - \mathbf{f}^{\text{ext},e}(t) \right] = 0 \\ \mathbf{f}^{\text{int},e}(t) = \int_{\Omega^e} \bar{\mathbf{B}}^T \boldsymbol{\sigma}(t) d\Omega^e, \quad t \in [0, T] \end{aligned} \quad (68)$$

where $(\cdot)^{\text{ext},e}$ and $(\cdot)^{\text{int},e}$ denotes respectively, the element contributions towards external and internal force vector whereas Ω^e is the element domain. The parameter t in (68) is the pseudo-time which is used to describe the particular loading program, which is typically described by an incremental sequence.

In the strain hardening phase, the complete response and the corresponding value of stress $\boldsymbol{\sigma}(t)$ in (68) can be obtained only if the evolution of plastic strains $\bar{\boldsymbol{\varepsilon}}^P(t)$ and hardening variable $\bar{\boldsymbol{\xi}}(t)$ is known.

The latter can be obtained one incremental step at the time by integrating the rate equations in (40) such that the loading/unloading conditions in (41) remain satisfied. If the backward Euler is used for this kind of integration (Bathe 1996 or Simo and Hughes 2000), one can compute the evolution of the plastic strains and hardening variable over any time interval $\Delta t = t_{n+1} - t_n$ with:

$$\bar{\boldsymbol{\varepsilon}}_{n+1}^P = \bar{\boldsymbol{\varepsilon}}_n^P + \bar{\gamma}_{n+1} \frac{\partial \bar{\phi}}{\partial \boldsymbol{\sigma}_{n+1}} \quad (69)$$

$$\bar{\boldsymbol{\xi}}_{n+1} = \bar{\boldsymbol{\xi}}_n + \bar{\gamma}_{n+1}$$

which further implies that the corresponding stress evolution reads:

$$\boldsymbol{\sigma}_{n+1} = \boldsymbol{\sigma}_n + \mathbf{C} \left(\Delta \boldsymbol{\varepsilon}_{n+1} - \bar{\gamma}_{n+1} \frac{\partial \bar{\phi}}{\partial \boldsymbol{\sigma}_{n+1}} \right) \quad (70)$$

The plastic multiplier $\bar{\gamma}_{n+1}$ in (69) and (70) is computed from plastic admissibility condition:

$$\bar{\gamma}_{n+1} > 0; \quad \bar{\phi}(\bar{\gamma}_{n+1}) = 0 \quad (71)$$

It is very important to note that the computations described in (69) to (71) are carried out independently from one quadrature point to another for the chosen numerical integration rule (e.g. 2×2 Gauss quadratic, see Hughes 1987 or Bathe 1996) which is employed to compute the internal force integral in (68). The main result of such a computation which is needed at the global level for solving the set of equilibrium equation in (68) is the plastically admissible value of stress in (70), as well as the elasto-plastic tangent modulus of the discrete problem:

$$\begin{aligned} \mathbf{C}_{n+1}^{\text{ep}} = \frac{\partial \boldsymbol{\sigma}_{n+1}}{\partial \bar{\boldsymbol{\varepsilon}}_{n+1}} = \mathbf{C} - \frac{2\mu}{\left(1 + \frac{\bar{\mathbf{K}}}{3\mu}\right) \|\mathbf{s}\|^2} \mathbf{s} \otimes \mathbf{s} \\ - \frac{(2\mu)^2 \bar{\gamma}_{n+1}}{\|\mathbf{s}_n + 2\mu \Delta e_{n+1}\|} \left[\mathbf{I} - \frac{1}{\|\mathbf{s}_{n+1}\|^2} \mathbf{s}_{n+1} \otimes \mathbf{s}_{n+1} \right. \\ \left. - \frac{1}{3} \mathbf{1} \otimes \mathbf{1} \right] \end{aligned} \quad (72)$$

Equivalent computations are carried out in strain softening phase, which is started once the localization condition in (50) happens to be verified for one of the quadrature points. One can thus obtain that:

$$\bar{\phi}(\bar{\gamma}_{n+1}) = 0; \quad t_{m,n+1} = t_y - \bar{\mathbf{q}}(\bar{\boldsymbol{\xi}}_{n+1}) \quad (73)$$

$$\bar{\mathbf{K}}_{n+1} = - \frac{d\bar{\mathbf{q}}}{d\bar{\boldsymbol{\xi}}_{n+1}} \quad (74)$$

Having presented the time evolution computations for both types of plastic response, hardening and softening, we now turn towards our main concern in the finite element implementation which is the choice of the discrete approximation of displacement field or the choice of element type. Two problems ought to be addressed in this respect: first, the locking phenomena in plastic hardening behavior of quasi-incompressible type, which occurs for given choice of von Mises yield criterion rendering the plastic deformation incompressible (Nagtegaal et al. 1974) and second the displacement discontinuity representation in the finite element setting. To that end, we introduce the mixed-enhanced strain field, which, on one side, introduces the independent volume-change deformation measure $\theta(\mathbf{x})$ and, on the other side, the displacement discontinuity mode producing purely deviatoric strain field.

In particular, the general expression for strain field in (56) over each mixed-enhanced finite element can be written as:

$$\boldsymbol{\varepsilon} = \mathbf{dev}[\mathbf{V}^s \mathbf{u}] + \frac{1}{3} \theta \mathbf{1} + \tilde{\mathbf{G}} \bar{\boldsymbol{\eta}} + \bar{\boldsymbol{\eta}} (\mathbf{m} \otimes \mathbf{n})^s \delta_{\Gamma_s}, \quad (75)$$

where $\mathbf{dev}[\mathbf{V}^s \mathbf{u}] = (\mathbf{I} - \frac{1}{3} \mathbf{1} \otimes \mathbf{1}) \mathbf{V}^s \mathbf{u}$.

In (75) and the rest of this section subscript ' $n + 1$ ' is dropped in order to simplify the notation. The strain energy can be split accordingly into:

$$\psi(\mathbf{u}, \theta, \bar{\boldsymbol{\varepsilon}}^p, \bar{\boldsymbol{\xi}}, \bar{\boldsymbol{\xi}}) = \bar{\psi}(\mathbf{dev}[\mathbf{V}^s \mathbf{u}] - \bar{\boldsymbol{\varepsilon}}^p, \bar{\boldsymbol{\xi}}) + U(\theta) + \bar{\bar{\psi}}(\bar{\boldsymbol{\xi}}) \delta_{\Gamma_s}, \quad (76)$$

If the plastically admissible values of stress and internal variables are provided as given previously in (69) to (74), one write the corresponding form of the total potential energy:

$$\begin{aligned} \Pi(\mathbf{u}, \theta, p, \bar{\boldsymbol{\varepsilon}}^p, \bar{\boldsymbol{\xi}}, \bar{\boldsymbol{\xi}}) = & \frac{\text{Nel}}{\text{A}} \left\{ \int_{\omega^e} \bar{\psi}(\mathbf{dev}[\mathbf{V}^s \mathbf{u}] - \bar{\boldsymbol{\varepsilon}}^p, \bar{\boldsymbol{\xi}}) \right. \\ & + U(\theta) + p(\text{tr}[\mathbf{V}^s \mathbf{u}] - \theta) d\Omega \\ & \left. + \int_{\Gamma_s} \bar{\bar{\psi}}(\bar{\boldsymbol{\xi}}) ds \right\} \quad (77) \end{aligned}$$

where p is the pressure which plays the role of Lagrange multiplier. Keeping the internal variables fixed, we can obtain from (77) the variational equations by appealing to the Gâteaux derivative formalism:

$$\begin{aligned} 0 = D_{\mathbf{u}} \Pi(\cdot) \cdot \delta \mathbf{u} = & \frac{\text{Nel}}{\text{A}} \int_{\Omega^e} [\mathbf{dev}[\boldsymbol{\sigma}] \cdot \mathbf{dev}[\mathbf{V}^s \delta \mathbf{u}]] \\ & + p \underbrace{\text{tr}[\mathbf{V}^s \delta \mathbf{u}]}_{\text{div}[\delta \mathbf{u}]} d\Omega - \delta \Pi_{\text{ext}} \quad (78) \end{aligned}$$

along with

$$0 = D_p \Pi(\cdot) \cdot \delta p = \int_{\Omega^e} [\delta p \cdot \text{div}[\mathbf{u}] - \theta] d\Omega; \quad \mathbf{e} \in [1, \text{Nel}] \quad (79)$$

and

$$0 = D_{\theta} \Pi(\cdot) \cdot \delta \theta = \int_{\Omega^e} \left[\delta \theta \cdot \left(-p + \frac{dU}{d\theta} \right) \right] d\Omega; \quad \mathbf{e} \in [1, \text{Nel}] \quad (80)$$

where $\delta \mathbf{u}$, δp and $\delta \theta$ are the corresponding variations of displacement, pressure and volume-change fields.

Within the framework of the finite element approximation, one can construct the following representations of the real and virtual displacement fields and their derivatives.

$$\mathbf{u}(\mathbf{x})|_{\Omega^e} = \sum_{\mathbf{e}=1}^{\text{Nel}} N_a(\mathbf{x}) \mathbf{u}_a; \quad \delta \mathbf{u}(\mathbf{x})|_{\Omega^e} = \sum_{\mathbf{e}=1}^{\text{Nel}} N_a(\mathbf{x}) \delta \mathbf{u}_a$$

$$\text{Nel} = 4 : N_a(\mathbf{x}) = \frac{1}{4} (1 + \xi_a \xi)(1 + \eta_a \eta); \quad \xi_a, \eta_a = \pm 1$$

$$\nabla^s \delta \mathbf{u}(\mathbf{x})|_{\Omega^e} = \sum_{\mathbf{e}=1}^{\text{Nel}} B_a(\mathbf{x}) \delta \mathbf{u}_a; \quad B_a(\mathbf{x}) = \nabla^s N_a$$

$$\mathbf{div}[\mathbf{u}]|_{\Omega^e} = \mathbf{b}^T(\mathbf{x}) \mathbf{u}$$

(81)

where \mathbf{u}_a and $\delta \mathbf{u}_a$ are the corresponding nodal values of the real and virtual displacement fields, and $N_a(\mathbf{x})$ are the displacement shape functions.

It is important to note that the variational equation in (78) requires that the shape function N_a be continuous across element boundaries, and (81) indicates one such choice given for a 4-node quadrilateral element in terms of its natural coordinates ξ and η (see Hughes 1987 or Bathe 1996). The same restriction of continuity does not apply to other fields featuring in variational equations (78) to (80) so that we can choose:

$$\begin{aligned} \theta(\mathbf{x})|_{\Omega^e} &= \mathbf{I}^T \boldsymbol{\theta}; \quad \delta \theta(\mathbf{x})|_{\Omega^e} = \mathbf{I}^T \delta \boldsymbol{\theta} \\ p(\mathbf{x})|_{\Omega^e} &= \mathbf{I}^T p; \quad \delta p(\mathbf{x})|_{\Omega^e} = \mathbf{I}^T \delta p \end{aligned} \quad (82)$$

where $\boldsymbol{\theta}$ and \mathbf{p} are the volume-change and pressure field interpolation parameters defined in each element independently from others.

By replacing the approximations defined in (81) and (82) into variational equations, (79) and (80) we obtain, respectively, alternative representation for volume-change and pressure field as:

$$\begin{aligned} \delta \mathbf{p}^T \underbrace{\int_{\Omega^e} \mathbf{1} \otimes \mathbf{1} d\Omega}_{\mathbf{L}} \theta &= \delta \mathbf{p}^T \int_{\Omega^e} \mathbf{1} \otimes \mathbf{b} d\Omega \mathbf{u} \Rightarrow \theta|_{\Omega^e} \\ &= \bar{\mathbf{b}}_a(\mathbf{x}) \mathbf{u}_a; \quad \bar{\mathbf{b}}(\mathbf{x}) = \mathbf{L}^{-1} \int_{\Omega^e} \mathbf{1} \otimes \mathbf{b} d\Omega \end{aligned} \quad (83)$$

and

$$\begin{aligned} \delta \boldsymbol{\theta}^T \int_{\Omega^e} \mathbf{1} \otimes \mathbf{1} d\Omega p &= \delta \boldsymbol{\theta}^T \int_{\Omega^e} \mathbf{1} \frac{dU}{d\theta} d\Omega \Rightarrow p|_{\Omega^e} \\ &= \mathbf{L}^{-1} \int_{\Omega^e} \mathbf{1} \frac{dU}{d\theta} d\Omega \end{aligned} \quad (84)$$

Moreover, we can easily show that the following orthogonality condition is valid:

$$\begin{aligned} p\mathbf{1} \cdot \mathbf{B}^{\text{dev}}\mathbf{u} &= 0; \quad \text{dev}[\boldsymbol{\sigma}] \cdot \mathbf{B}^{\text{vol}} = 0 \\ \mathbf{B}^{\text{dev}} &= \left(\mathbf{I} - \frac{1}{3}\mathbf{1} \otimes \mathbf{1} \right) \mathbf{B}; \quad \mathbf{B}^{\text{vol}} = \left(\frac{1}{3}\mathbf{1} \otimes \mathbf{1} \right) \mathbf{B} = \frac{1}{3}\mathbf{1} \otimes \mathbf{b}; \\ \mathbf{B} &= \mathbf{B}^{\text{dev}} + \mathbf{B}^{\text{vol}} \end{aligned} \quad (85)$$

We can recast the variational equation in (78) according to:

$$\begin{aligned} 0 &= \sum_{e=1}^{\text{Nel}} \int_{\Omega^e} \mathbf{B}^{\text{dev}} \cdot \text{dev}[\boldsymbol{\sigma}] + \mathbf{B}^{\text{vol}} \cdot \bar{p}\mathbf{1} \, d\Omega - \mathbf{f}^{\text{ext},e} \\ &= \sum_{e=1}^{\text{Nel}} \int_{\Omega^e} \bar{\mathbf{B}} \cdot \boldsymbol{\sigma} \, d\Omega - \mathbf{f}^{\text{ext},e} \end{aligned} \quad (86)$$

with

$$\bar{\mathbf{B}}^{\text{vol}} = \frac{1}{3}\mathbf{1} \otimes \bar{\mathbf{b}}; \quad \bar{\mathbf{B}} = \mathbf{B}^{\text{dev}} + \bar{\mathbf{B}}^{\text{vol}}; \quad \boldsymbol{\sigma} = \text{dev}[\boldsymbol{\sigma}] + \bar{p}\mathbf{1} \quad (87)$$

Hence, the final form of the variational equation in (86) above allows us to construct independently from the given displacement approximations the finite element approximation of the volume-change strain field; which able to avoid the quasi-incompressibility induced locking phenomena (e.g. see Hughes 1987) which are also typical of von Mises plasticity (e.g. see Nagtegaal et al. 1974). One possible choice of locking-free finite element approximation which is employed in the foregoing is given for a 4-node quadrilateral element with displacement field represented by bi-linear polynomials as indicated in (81), combined with element-wise constant representation of volume-change and pressure fields, so that the result in (83) will simplify to:

$$\bar{\mathbf{b}} = \frac{1}{\Omega^e} \int_{\Omega^e} b \, d\Omega \quad (88)$$

In the strain softening phase, once it is triggered by the localization criterion verification within a particular element Ω^e , we ought to construct the enhanced representation of the displacement field which is capable of capturing the discontinuity. As indicated in (50) and (52), the localization condition sets the orientation of the shear band in terms of the corresponding unit vector \mathbf{n} . In accordance to the strain in (75) it holds that the plastic deformation along discontinuity should remain purely deviatoric, which gives that \mathbf{n} and \mathbf{m} are initially orthogonal. With discontinuity induced plastic deformation which is purely deviatoric, we can keep the same form of the mixed variational principle and the resulting B-bar strain representation as indicated in (86).

The discontinuity can be introduced in two different manners separating either only one node from the remaining 3 nodes of the quadrilateral element or splitting the 4-node quadrilateral in such a way that a pair of nodes is placed at each side of the discontinuity. If Ω^+ denotes

the part of the element on one side of the slip line, we can thus write:

$$M_{\Gamma_s^e}(\mathbf{x})|_{\Omega^e} = H_{\Gamma_s^e}(\mathbf{x}) - \sum_{b \in \Omega^+} N_b(\mathbf{x}) \quad (89)$$

The corresponding form of the enhanced strain can be obtained by taking the derivative of the given displacement interpolation

$$\tilde{\boldsymbol{\epsilon}}|_{\Omega^e} = \tilde{\mathbf{G}}\bar{\boldsymbol{\eta}} + \bar{\boldsymbol{\eta}}(\mathbf{m} \otimes \mathbf{n})^s \delta_{\Gamma_s} \quad (90)$$

where

$$\begin{aligned} \tilde{\mathbf{G}} &= \sum_{b \in \Omega^+} \bar{\mathbf{B}}_b^{\text{dev}}(\mathbf{x})\mathbf{m} - \frac{1}{\Omega^e} \int_{\Omega^e} \sum_{b \in \Omega^+} \bar{\mathbf{B}}_b^{\text{dev}}(\mathbf{x})\mathbf{m} \, d\Omega^e \\ &\quad + \frac{\ell_{\Gamma_s}}{\Omega^e} (\mathbf{m} \otimes \mathbf{n})^s \end{aligned} \quad (91)$$

We note that the chosen enhanced strain field satisfies the patch test. With this result on hand, we can rewrite the set of equilibrium equations in (86) as:

$$\begin{aligned} \mathbf{r} &= \sum_{e=1}^{\text{Nel}} \left[\int_{\Omega^e} \bar{\mathbf{B}} \cdot \boldsymbol{\sigma} \, d\Omega - \mathbf{f}^{\text{ext}} \right] = 0 \\ \mathbf{h}^e &= \int_{\Omega^e} \tilde{\mathbf{G}} \cdot \boldsymbol{\sigma} \, d\Omega + \int_{\Gamma_s} \bar{\boldsymbol{\eta}}\mathbf{m} \cdot \mathbf{t} \, d\Gamma = 0, \quad e \in [1, \text{Nel}] \end{aligned} \quad (92)$$

where the supplementary equation expresses the weak form equilibrium over particular element Ω^e with respect to the variation of enhanced strains.

Such a structure of the system allows us to reduce the problem to the original size in (86) without the incompatible modes, by appealing to the static condensation procedure (e.g. see Ibrahimbegovic et al. 1998).

4 Numerical examples

In this section, we present the results of several numerical simulations of a failure process by shear banding which serve to further illustrate the main features of the proposed methodology. All the computations are carried out by the computer program *FEAP*, which is developed by Professor R.L. TAYLOR at UC Berkeley (e.g. see Zienkiewicz Taylor 2000). The finite element models all employ the 4-node quadrilateral element with $\bar{\mathbf{B}}$ strain interpolations and embedded discontinuity.

4.1 Pure shear test

We present here some results obtained considering a very simple test with a reduce number of elements in order to test the capabilities of the model. The test considered is a pure shear one as presented in Fig. 2. The material properties are given in Table 1.

The problem is solved using the arclength method. In order to change the bifurcation problem into a localization one, a band of elements (in gray in Fig. 2) has been weakened by slightly reducing the limit stress. The

sensitivity of the proposed model to mesh refinement and mesh distortion is checked by considering the different meshes presented in Fig. 2.

The results are given in Fig. 3 in terms of the horizontal shear load versus the horizontal displacement of point A. We can note that, as expected, the numerical results are quite independent of mesh refinement and distortion.

4.2 Simple shear test

In this example, we consider a simple shear test under plane strain condition. The test is carried out under displacement control: horizontal displacements at top and bottom of the specimen are imposed as indicated in Fig. 4 (rotations are not allowed). The analysis is carried out considering a J2 plasticity model with an exponential hardening rule with saturation and a linear softening rule. The material considered is quasi incompressible, its characteristics are given in Table 2. The tested sample is a rectangular of 20 cm long and 10 cm high.

As for the test presented here above, in order to control localization, a band of elements (in gray on Fig. 4) is weakened by slightly reducing the limit stress. Mesh objectivity is checked considering different mesh refinements. The results are depicted in Fig. 5 in terms of the horizontal load versus the imposed displacement for two different mesh refinements.

It can be noted that the results in terms of the limit load and the dissipated energy are quite identical. We can also note that, in the case of quasi-incompressible material, the use of the B-bar method solve efficiently the problem of locking.

Table 1. Material properties for pure shear test

Continuum plasticity model	
Young modulus	210 GPa
Poisson ratio	0.4999
σ_y	0.35 GPa
σ_∞	0.60 GPa
β	200
Softening rule parameter	
\bar{K}	-0.05 GPa/mm

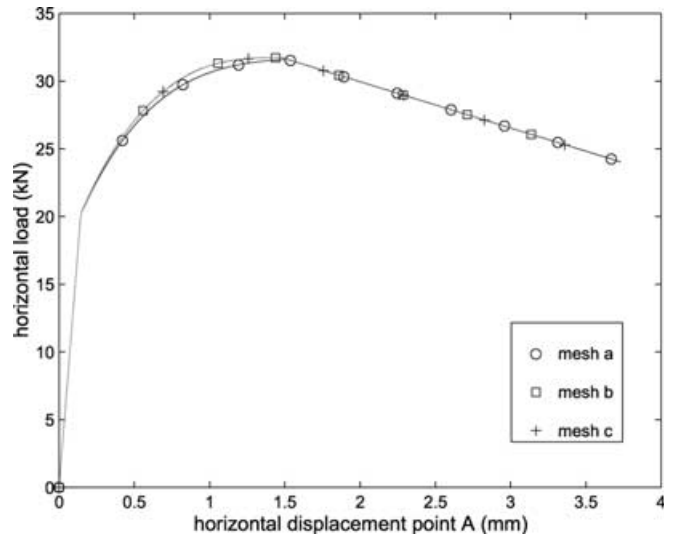


Fig. 3. Load/displacement results for a pure shear test

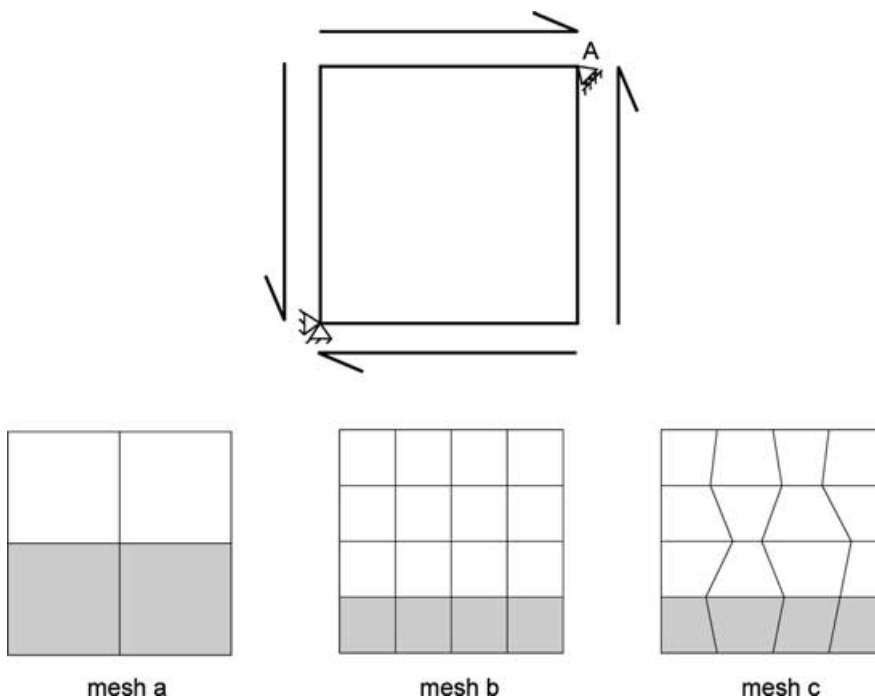


Fig. 2. Pure shear test

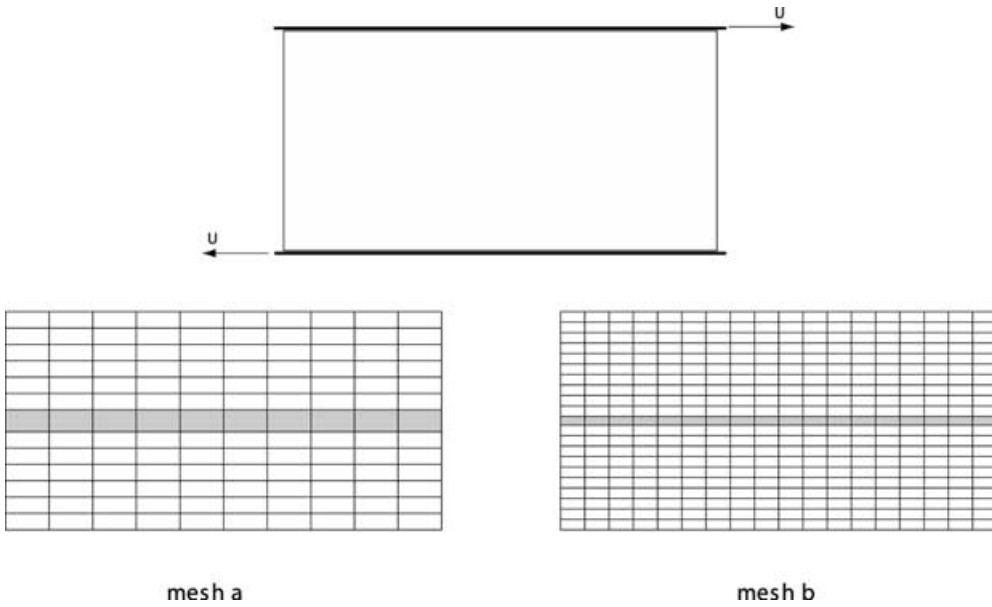


Fig. 4. Simple shear test

4.3

Traction test

We present here some results considering a double notched beam submitted to a traction test under plain strain condition (see Fig. 6). The material parameters are the same then those used for the simple shear test presented here above (see Table 2).

Table 2. Material properties for simple shear test

Continuum plasticity model	
Young modulus	210 GPa
Poisson ratio	0.4999
σ_y	0.55 GPa
σ_∞	0.75 GPa
β	200
Softening rule parameter	
\bar{K}	-0.1 GPa/mm

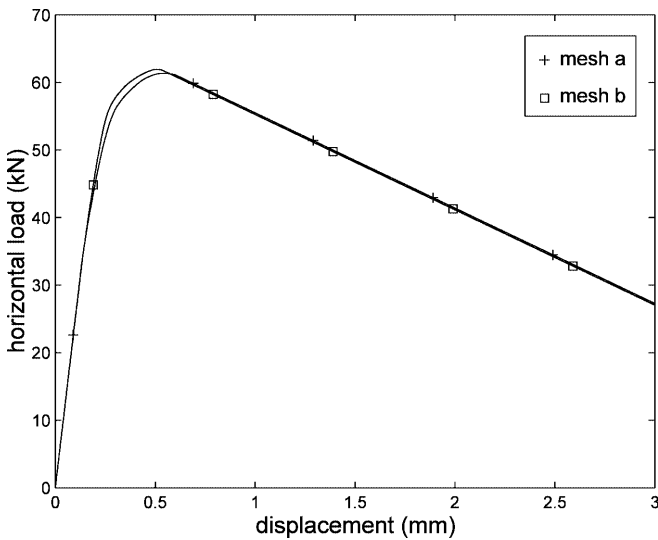


Fig. 5. Load/displacement results for a simple shear test

The test is carried out under displacement control. The tested sample is 20 cm long and 10 cm high. Figure 7 shows the map of accumulated plastic deformation at the end of the test. A shear band develops during the test between the two notches of the beam. Figure 8 gives a representation, at the end of the test, of the discontinuity lines activated in localized elements. A straightforward parallelism can be made between Fig. 7 and Fig. 8: localized elements correspond to those where plastic deformation has significantly developed. Those two figures

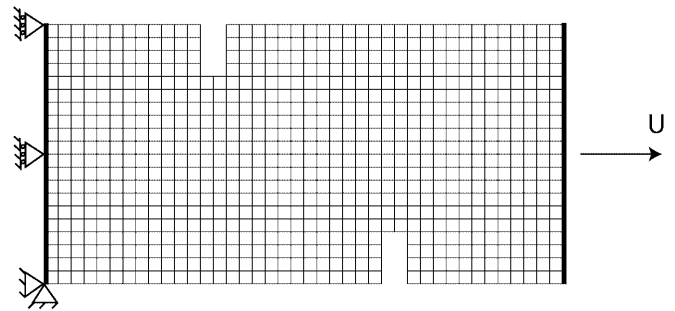


Fig. 6. Traction test

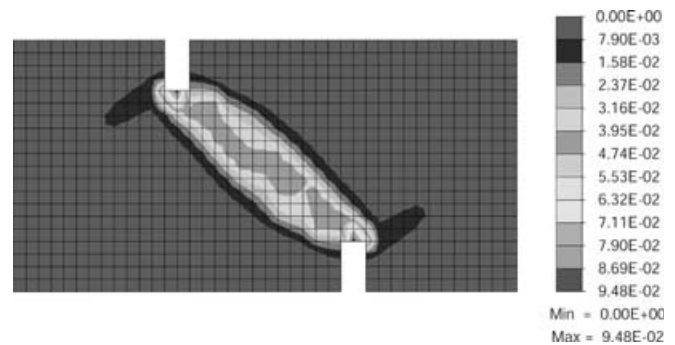


Fig. 7. Accumulated plastic deformation

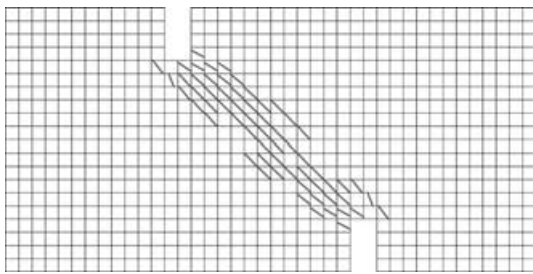


Fig. 8. Localized elements and discontinuity lines

illustrate the two different dissipative mechanisms taken into account by the model: a bulk dissipation mechanism characterized by the development of plastic deformation and a surfacic dissipation mechanism characterized by the creation of a displacement discontinuity.

5

Conclusions

In this work we developed a plasticity model where hardening mechanisms are combined in order to represent the plastic failure. The class of problem of main interest for this kind of model pertains to the failure of massive structures where final failure mechanism is preceded by significant development of plastic zone and where the contribution of the so-called fracture process zone remains of equal importance for total plastic dissipation as the actual failure mechanism itself. The case which is studied in detail is the plastic failure of metals where the plastic zone creation is governed by the von Mises yield criterion and where the failure mechanism is represented by plastic slip lines. This model problem requires that a special care be taken when choosing the finite element interpolations in order to eliminate the locking phenomena related to quasi-incompressible elasto-plastic response. The latter is achieved by using the \bar{B} mixed interpolations resulting with a development of a mixed-enhanced 4-node quadrilateral finite element, which also incorporates an embedded discontinuity as an enhanced mode which is activated at the start of the failure process. It is clear that the presented model would also possess the advantage over the vast majority of previous models of this kind which consider only elastic hardening and plastic softening in being able to predict better the final orientation of the shear slip line after the initial redistribution of the stress is completed. Additional advantage of this model with respect to other available models which choose so-called optimal SKON formulation (e.g. Jirásek 2000) is the choice of the real and virtual enhanced strains which are identical and thus guarantee the symmetry of the tangent operator and provides a more efficient computation procedure. Finally, although the chosen model problem considers only metals and the von Mises plasticity, the proposed concept of combining the inelastic hardening and inelastic softening to fully explain the failure of a massive structure can easily be adapted to other criteria and other models of inelastic response, such as damage or combined damage plasticity.

References

- Armiero F, Garikipati K (1995) Recent advances in the analysis and numerical simulation of strain localization in inelastic solids In: Owen E, Oñate DRJ, Hinton E (eds), Proceedings of Computational Plasticity IV, pp. 547–561 Barcelona, CIMNE
- Bathe KJ (1996) Finite element procedures Prentice Hall, New Jersey
- Bazant ZP, Belytschko TB, Chang TP (1984) Continuum theory for strain softening. *J. Eng. Mech.* 110(12): 1666–1691
- Belytschko T, Fish J, Engleman BE (1988) A finite element with embedded localization zones. *Comput. Meth. Appl. Mech. Eng.* 70: 59–89
- Belytschko T, Lasry D (1989) A Study of localization limiters for strain-softening in static and dynamics. *Comput. Struct.* 33(3): 707–715
- Coleman BD, Hodgdon ML (1985) On shear bands in ductile materials *Arch. Rati. Mech. Anal.* 90: 219–247
- Crisfield M (1997) Non linear finite element analysis of solids and structures, Vol. 1: Essentials. J. Wiley and sons, New York
- Crisfield M (1997) Non linear finite element analysis of solids and structures, Vol. 2: Advanced Topics. J. Wiley and sons, New York
- De Borst R, Sluys LJ (1991) Localisation in a cosserat continuum under static and dynamic loading conditions. *Comput. Meth. Appl. Mech. Eng.* 90: 805–827
- Hill R (1962) Acceleration waves in solids. *J. Mech. Phys. Solids.* 10: 1–16
- Hughes TJR (1987) The finite element methods. Prentice-Hall, Englewood-Cliffs, NJ, USA
- Ibrahimbegovic A, Gharzeddine F, Chorfi L (1998) Classical plasticity and viscoplasticity models reformulated: theoretical basis and numerical implementation *Int. J. Numer. Meth. Eng.* 42: 1499–1535
- Ibrahimbegovic A, Wilson EL (1991) A modified method of incompatible modes. *Commun. Appl. Numer. Meth.* 7: 187–194
- Jirásek M (2000) Comparative study on elements with embedded discontinuities. *Comput. Meth. Appl. Mech. Eng.* 188: 307–330
- Jirasek M, Zimmermann T (2001) Embedded crack model: Basic formulation. *Int. J. Numer. Meth. Eng.* 50: 1269–1290
- Lubliner J (1990) Plasticity theory. Macmillan, New York
- Luenberger D (1984) Linear and nonlinear programming. Addison-Wesley, Reading, MA
- Mandel J (1996) Conditions de Stabilité et postulat de drucker. In: Kravtchenko J, Sirieys PM (eds) Rheology and Soil Mechanics, Grenoble 1964. IUTAM Symposium
- Maugin GA (1992) The thermodynamics of plasticity and fracture. Cambridge University Press, Cambridge
- Nagtegaal JC, Parks DM, Rice JR (1974) On numerically accurate finite element solutions in the fully plastic range. *Comput. Meth. Appl. Mech. Eng.* 4: 153–178
- Needleman A (1988) Material rate dependence and mesh sensitivity in localization problems. *Comput. Meth. Appl. Mech. Eng.* 63: 69–85
- Oliver J (1995) Continuum modelling of strong discontinuities in solid mechanics. In: Fourth International Conference On Computational Plasticity, pp. 455–480 Barcelona
- Ortiz M, Leroy Y, Needleman A (1987) A finite element method for localized failure analysis. *Comput. Meth. Appl. Mech. Eng.* 61: 189–214
- Qiu Y, Crisfield MA, Alfano G (2001) An interface element formulation for the simulation of delamination with buckling. *Eng. Frac. Mech.* 68: 1755–1776
- Rice JR (1976) The localization of plastic deformation. In: Theor. and Applied Mechanics pp. 207–220. Proceedings of the 14th IUTAM Congress, Delft, North-Holland, Amsterdam
- Runesson K, Ottosen NS, Peric D (1991) Discontinuous bifurcations of elastic-plastic solutions at plane stress and plane strain. *Int. J. Plast.* 7: 99–121

- Simo JC, Hughes TJR** (2000) Computational inelasticity. Springer Verlag, Berlin
- Simo JC, Oliver J, Armero F** (1993) An analysis of strong discontinuity induced by strain softening solutions in rate-independent solids. *J. Comput. Mech.* 12: 277–296
- Stakgold I** (1979) Green's functions and boundary value problems. Wiley, London
- Strang G** (1986) Introduction to applied mathematics. Wellesley-Cambridge Press, Cambridge
- Truesdell C, Noll W** (1965) The Non-Linear Field Theories. Springer, Berlin
- Zienkiewicz OC, Taylor RL** (2000) The Finite Element Method. (5th edn) Butterworth-Heinemann, Oxford, UK